Author Manuscript

Author Manuscript

Author Manuscript

Author Manuscript

HHS Public Access

Author manuscript

Immunohorizons. Author manuscript; available in PMC 2022 July 26.

Published in final edited form as:

Immunohorizons. ; 6(6): 366–372. doi:10.4049/immunohorizons.2200019.

RXRα Regulates the Development of Resident Tissue Macrophages

Jordan Philpott[*,1], **Simon Kazimierczyk**[*,1], **Parimal Korgaonkar**[†], **Evan Bordt**[‡,§], **Jaclyn Zois**[*], **Chithirachelvi Vasudevan**[*], **Di Meng**[*], **Ishan Bhatia**[*], **Naifang Lu**[†], **Brittany Jimena**[*], **Caryn Porter**[†], **Bobby J. Cherayil**[*,§], **Nitya Jain**[*,†,§]

[*]Mucosal Immunology and Biology Research Center, Mass General Hospital for Children, Charlestown, MA

[†]Center for Computational and Integrative Biology, Massachusetts General Hospital, Boston MA

[‡]Lurie Center for Autism, Mass General Hospital for Children, Charlestown, MA 02129

[§]Department of Pediatrics, Harvard Medical School, Boston, MA

Abstract

Resident tissue macrophages (RTMs) develop from distinct waves of embryonic progenitor cells that seed tissues before birth. Tissue-specific signals drive a differentiation program that leads to the functional specialization of RTM subsets. Genetic programs that regulate the development of RTMs are incompletely understood, as are the mechanisms that enable their maintenance in adulthood. In this study, we show that the ligand-activated nuclear hormone receptor, retinoid X receptor (RXR)α, is a key regulator of murine RTM development. Deletion of RXRα in hematopoietic precursors severely curtailed RTM populations in adult tissues, including the spleen, peritoneal cavity, lung, and liver. The deficiency could be traced to the embryonic period, and mice lacking RXRα in hematopoietic lineages had greatly reduced numbers of yolk sac and fetal liver macrophages, a paucity that persisted into the immediate postnatal period.

INTRODUCTION

Macrophages are a heterogeneous population of cells that protect against infection and perform critical functions in organ development and tissue homeostasis (1). Murine resident tissue macrophages (RTMs) are represented by ontogenetically distinct populations that arise from distinct waves of precursor cells originating in the yolk sac (YS) and the aorta-gonadmesonephros region of the embryo. RTM identity is also shaped by residency, the duration of residency in tissues, and the influence of local environmental signals on

This article is distributed under the terms of the CC BY-NC-ND 4.0 Unported license.

Address correspondence and reprint requests to: Dr. Nitya Jain, Mucosal Immunology and Biology Research Center, Mass General Hospital for Children, 114 16th Street, Charlestown, MA 02129. njain@ccib.mgh.harvard.edu.

[1]J.P. and S.K. contributed equally to this work.

J.P., S.K., P.K., and N.J. performed experiments with help from E.B., J.Z., C.V., D.M., I.B., N.L., and B.J. C.P. managed the mouse colony B.J.C. helped in data interpretation. N.J. designed experiments and wrote the manuscript with input from authors.

DISCLOSURES

The authors have no financial conflicts of interest.

Author Manuscript Author Manuscript Author Manuscript Author Manuscript

epigenetic and transcriptional programs (2, 3). The origins of RTMs and tissue-specific factors that define and maintain RTM identity are incompletely understood.

Retinoid X receptor (RXR)α is a transcription factor that undergoes obligate heterodimerization with other members of the nuclear hormone receptor superfamily and has been implicated in the control of numerous physiological processes, including cell cycle, lipid and glucose metabolism, and immune responses (4, 5). RXRα has been previously shown to be important for proper macrophage function (6-9). More recently, RXRα was shown to regulate the homeostasis of embryonically derived serous cavity macrophages (10). This study concluded that RXRs do not control the fetal development of large peritoneal macrophages, but rather their postnatal expansion. In our study, selective ablation of *Rxra* from panhematopoietic cells through the use of a Cre recombinase under the control of the *Vav* promoter revealed impaired generation of YS and fetal liver (FL) macrophages but not FL hematopoietic stem cell (HSC)–derived monocyte populations, suggesting a role for RXRα in the embryonic development of RTMs.

MATERIALS AND METHODS

Animal care

Mouse studies were conducted under protocols approved by the Institutional Animal Care and Use Committee of Massachusetts General Hospital. *Rxra*$^{fl/fl}$ (stock no. 013086) and *Vav*-iCre (stock no. 008610) mice on the C57BL/6 background were purchased from The Jackson Laboratory and housed in HPPF facilities (*Heliobacter*- and *Pasteurella pneumotropica*–free).

Cell isolation

Single-cell preparations from various tissues were performed as described in Liu et al. (11). Briefly, 8- to 10-wk-old mice were euthanized and peritoneal lavage was collected and stored on ice. Mice were then perfused and tissues harvested into ice-cold PBS. Spleens were homogenized using a motored tissue homogenizer, and RBCs were lysed using ACK lysis buffer. Colon and small intestine were washed in EDTA containing buffer to remove epithelial fraction before Liberase (Roche, catalog no. 5401020001) digestion. Skin, liver, and lungs were also digested in Liberase and subjected to Percoll gradient centrifugation at 600 × *g* for 20 min to enrich for hematopoietic cells. Brain tissues were digested in an enzyme mix of collagenase A (MilliporeSigma, catalog no. 11088793001) and DNase I, grade II, from bovine pancreas (MilliporeSigma, Cat No. 10104159001) and cleaned of debris (Miltenyi Biotec, 130-109-398). Embryonic tissues (FL and YS) were homogenized between frosted glass slides and digested in Liberase TL (thermolysin low). Cells isolated from all tissues were counted in a Countess 3 (Thermo Fisher Scientific) counter and resuspended in FACS buffer in preparation for staining.

Iron and IBA-1 staining

Ferric iron deposits were visualized by Prussian blue staining of formalin-fixed, paraffin-embedded tissues. Multiple images of each biological replicate were taken using a 20× objective on a Nikon Eclipse 80i (Nikon, Tokyo, Japan). For IBA-1 staining, heat-mediated

Author Manuscript Author Manuscript Author Manuscript Author Manuscript

Ag retrieval with Tris/EDTA buffer was performed on paraffin-embedded spleen tissues followed by blocking in goat serum containing 0.3% Triton X-100. IBA-1 was stained using rabbit monoclonal anti–IBA-1 (Abcam, ab178847) primary Ab at 1:500 dilution followed by Alexa Fluor 488–conjugated goat anti-rabbit IgG (ab150077) at 1:1000 dilution. Images were taken using a Zeiss Imager Z1 (Zeiss, Thornwood, NJ).

Flow cytometry

A maximum of 3×10^6 cells were stained with fluorescent dye–conjugated Abs as described previously (12). Samples were acquired on a custom-made LSRFortessa X-20, and data were analyzed using FlowJo software (Tree Star). Changes in Ab staining panels (e.g., Ab clones and reagent batches) across experiments were minimized. Strong discrepancies in staining from different experiments were noted, and the data in question were excluded from final analyses.

Abs for flow cytometry

The following Abs were used for flow cytometry: CD115 Alexa Fluor 488 (AFS98, BioLegend, 135512), CD93 PerCP-Cy5.5 (AA4.1, BioLegend, 136512), CD144 PE (11D4.1, BD Biosciences, 562243), F4/80 PE-CF594 (T45-2342, BD Biosciences, 565613), CD64 PE-Cy7 (X54-5/7.1, BioLegend, 139314), Sca-1 allophycocyanin (D7, BioLegend, 108112), CD16/32 allophycocyanin-R700 (2.4G2, BD Biosciences, 565502), CD11c allophycocyanin-780 (N418, eBio-science, 47011482), CD41 BV421 (MWReg30, BD Biosciences, 747729), Ter119 BV510 (TER-119, BD Biosciences, 563995), Ly6G BV605 (1A8, BD Biosciences, 563005), CX3CR1 BV650 (SA011F11, BioLegend, 149033), c-Kit BV711 (2B8, BD Biosciences, 105835), CD45 BV786 (30-F11, BD Biosciences, 564225), CD3e BUV395 (145-2C11, BD Biosciences, 563565), CD11b BUV737 (M1/70, BD Biosciences, 564443), CD68 PerCP-Cy5.5 (FA-11, BioLegend, 137010), VCAM1 Alexa Fluor 647 (429, BioLegend, 105712), MHC class II Alexa Fluor 700 (M5/114, Thermo Fisher Scientific, 56532182), Siglec-F BV421 (E50-2440, BD Biosciences, 562681), Tim-4 BV510 (21H12, BD Biosciences, 742774), Live/Dead, fixable UV (Thermo Fisher Scientific, L34962).

Statistical analysis

For comparison between two cohorts, a minimum of four mice per group was used, and the experiments were repeated at least twice. The D'Agostino and Pearson omnibus normality test was used to determine whether values came from a Gaussian distribution. A two-tailed unpaired *t* test was used to calculate significance in the comparisons of two cohorts that were normally distributed. A Mann–Whitney *U* test was performed for comparing groups that failed normality tests. Graphs are vertical scatter plots showing the SEM. Animals of both sexes were used as available. No randomization was performed, and investigators were not blinded to group allocations.

Author Manuscript Author Manuscript Author Manuscript Author Manuscript

RESULTS

RXRα deficiency alters multiple RTM populations

We deleted RXRα in developing precursor cells by crossing *Rxra*$^{fl/fl}$ mice (13) with *Vav*-iCre transgenic mice (14, 15). *Vav* expression is restricted to hematopoietic cells and is reported in CD45^{+}VEC^{-} cells of the aorta-gonad-mesonephros region and FL at embryonic day (E)11.5 (15, 16). To minimize germline deletion of the floxed allele, male *Rxra*$^{fl/fl}$ mice were mated with female *Vav*$^{Cre+}$*Rxra*$^{fl/fl}$ mice, and PCR-genotyped adult littermate progeny were used for analyses. RXRα deficiency had no impact on total splenic cellularity or the distribution of splenic B and T cell subsets (Supplemental Fig. 1). However, we noted a lack of F4/80^{hi}VCAM1^{+} splenic red pulp macrophages and bone marrow erythroblastic island macrophages in *Vav*$^{Cre+}$ *Rxra*$^{fl/fl}$ mice compared with control RXRα$^{fl/fl}$ mice (Fig. 1A, 1C). Immunohistochemistry staining of spleen with the pan-macrophage marker, IBA-1, confirmed this phenotype (Fig. 1B, top row). Red pulp macrophages are critical for phagocytosis of senescent RBCs and iron recycling, and in their absence, *Vav*$^{Cre+}$*Rxra*$^{fl/fl}$ mice accumulated ferric iron in the spleen (Fig. 1B, bottom row). This phenotype was similar to that of *Vav*$^{Cre+}$*Pparg*$^{fl/fl}$ mice (17), an observation of potential significance in the present context because PPARγ is a binding partner of RXRα. PPARγ was initially identified as a transcription factor critical for perinatal alveolar macrophage development (18, 19). Adult *Vav*$^{Cre+}$*Rxra*$^{fl/fl}$ mice also had severely reduced CD11c^{+}Siglec-F^{+} lung alveolar macrophage populations and IBA-1^{+} cells (Fig. 1D, 1E). Given the shared embryonic origins of RTM subsets, we interrogated RTMs in other tissues of adult *Vav*$^{Cre+}$*Rxra*$^{fl/fl}$ mice and found similar declines in liver F4/80^{+}Tim-4^{+} Kupffer cells, CD11b^{+}F4/80^{hi} large peritoneal cavity macrophages, and a small but significant reduction in small intestinal CD11b^{+}CD64^{+} gut macrophages (Fig. 1F-H). Colonic macrophages that are derived from circulating bone marrow monocytes were not impacted (Fig. 1I), as were brain CD45^{lo}CD11b^{+} microglia that arise from distinct primitive YS precursors at E7.5 (20) where RXRα is not expected to be deleted using the Vav-iCre strategy (Fig. 1J). Skin CD11b^{+}F4/80^{+} Langerhans cells, which derive from a mix of YS and FL cells (21), were not affected by RXRα deficiency (Fig. 1K). Thus, our data pointed to a role for RXRα in regulating homeostasis of select RTM subsets arising from embryonic precursors. Our observations contrast with a recent report of RXRα deletion in macrophages using *LysM*-Cre transgene that also showed a reduction in cavity and liver macrophages but not in any other tissues (10). This discrepancy is likely due to poor *LysM* promoter-driven Cre recombinase expression in macrophage precursors during embryonic development that may have resulted in inefficient deletion of RXRα (10, 18, 22).

RXRα deficiency impairs embryonic development of RTM precursors

RTMs arise from embryonic precursors that seed tissues where they undergo rapid expansion. These precursors have been proposed to include YS-derived erythromyeloid progenitors (EMPs) (23), “late” EMP-derived fetal monocytes (24), or HSC-derived fetal monocytes (25). The current paradigm is that *Csf1r*-expressing EMPs give rise to circulating macrophage precursors (pMacs) that colonize embryos at the onset of organogenesis from E9.5 (3, 23, 26). We therefore determined whether RXRα regulated the initial development of RTM subsets or their postnatal expansion. Analysis of a publicly available fetal

Author Manuscript Author Manuscript Author Manuscript Author Manuscript

macrophage dataset (3) revealed that *Rxra* transcripts may be detected as early as E9 in YS EMPs (Fig. 2A). Interestingly, *Vav1* expression was also found in these CD45^{lo}c-Kit^{+} EMPs, raising the possibility of *Rxra* deletion in YS precursors. We therefore analyzed YS tissue from E9.5 embryos of time-pregnant *Vav*$^{Cre+}$*Rxra*$^{fl/fl}$ females mated with *Rxra*$^{fl/fl}$ males (Fig. 2B, 2C). We noted considerable variability in the distribution of cell subsets at this embryonic stage, and although the frequency of CD45^{+}c-Kit^{+} EMPs trended higher in *Vav*$^{Cre+}$*Rxra*$^{fl/fl}$ embryos, significance was not achieved (Fig. 2B). However, our analysis did uncover significant deficits in CD45^{+} F4/80^{+} cells in E9.5 knockout embryos (Fig. 2B). Furthermore, CD45^{+}CD11b^{lo}F4/80^{-} pMacs and CD45^{+}CD11b^{+}F4/80^{+} macrophages were diminished in KO YS (Fig. 2C), suggesting either a block in transition from EMP to pMac/macrophage stage in the absence of RXRα or altered proliferation and/or apoptosis in pMacs. YS EMPs additionally migrate to the FL where they can differentiate into RTMs (27). *Vav*$^{Cre+}$*Rxra*$^{fl/fl}$ FL at E14.5 also contained significantly fewer CD11b^{lo}F4/80^{hi} macrophages but not CD11b^{hi}F4/80^{lo} monocytes compared with controls (Fig. 2D). In agreement with this embryonic deficit, there were negligible RTMs in the spleen, liver, and lungs of postnatal day 1 *Vav*$^{Cre+}$*Rxra*$^{fl/fl}$ mice, a paucity that persisted until postnatal day 8 (Fig. 2E). These data confirmed that the impairment in RTM homeostasis in RXRα-deficient animals began during embryonic development and was likely exacerbated by lack of expansion during the postnatal period.

DISCUSSION

Our studies position RXRα as a key regulator of early life RTM development. Murine RTMs are produced during three consecutive waves of hematopoietic development. The first wave, called primitive hematopoiesis, occurs in the YS at E7.5 and gives rise to microglia of the brain (20). In the *Vav*$^{Cre+}$ model of *Rxra* deletion, we noted no changes in adult microglia (Fig. 1J), and it remains to be determined, by the use of Cre systems that are activated earlier in ontogeny, whether RXRα might regulate aspects of this primitive developmental process. The second wave of macrophages arises from EMPs that are derived from hemogenic endothelium in the YS vasculature at E8.25 (28). In this wave of definitive hematopoiesis, YS EMPs generate circulating macrophage precursors that colonize embryonic tissues directly (3). EMPs may also migrate to the FL and give rise to fetal erythrocytes and myeloid cells including RTMs (27). *Vav*$^{Cre+}$*Rxra*$^{fl/fl}$ YS at E9.5 and FL at E14.5 contained fewer CD11b^{lo}F4/80^{-} macrophage precursors and negligible F4/80^{+} macrophages, respectively (Fig. 2B-D). These data suggested that RXRα might regulate developmental aspects of precursor macrophages that arise from EMPs. The third wave of macrophages arises from HSC-derived Sca-1^{+} monocytes (27). Similar to EMPs, HSCs are also derived from hemogenic endothelium and migrate to the FL at E10.5 and to the bone marrow at E17.5 where they give rise to monocytes and other lymphoid and myeloid cells. In *Vav*$^{Cre+}$*Rxra*$^{fl/fl}$ mice, this arm of monocyte-derived macrophage development appeared unperturbed (Fig. 1I, 1K), suggesting a unique requirement for RXRα in embryonic precursors to generate specific RTM subsets.

RXRα forms heterodimers with other nuclear receptor family members such as the retinoic acid receptor, the vitamin D receptor, and PPARγ, allowing for pleiotropic signaling (29). It is therefore intriguing to speculate that precursors, including EMPs, receive distinct

Author Manuscript Author Manuscript Author Manuscript Author Manuscript

extrinsic cues that feed into the RXRα signaling pathway and direct cells toward the RTM lineage. A function for RXRα in regulating migration of progenitors to embryonic tissues cannot also be ruled out, given that RXRα controls chemokine production in myeloid cells that affects leukocyte recruitment to inflammatory sites (7). In conclusion, we have uncovered an unexpected role for RXRα in the embryonic development of RTM subsets. Our observations will lead the way for future studies directed at identifying embryonic precursors that generate RTM subsets as well as understanding the role of tissue-specific ligands in directing RTM cell fate.

Supplementary Material

Refer to Web version on PubMed Central for supplementary material.

ACKNOWLEDGMENTS

We are thankful for the resources of the Center for Computational and Integrative Biology and the Mucosal Immunology and Biology Research Center at MGH that supported this study.

This work was supported by National Institutes of Health Grants 1R01 AI154626-01 and 1R21 AI153548-01 (to N.J.) and National Institutes of Health Grants R01 AI089700 and R21 AI155593 (to B.J.C.).

Abbreviations used in this article:

E	embryonic day
EMP	erythromyeloid progenitor
FL	fetal liver
HSC	hematopoietic stem cell
pMac	macrophage precursor
RTM	resident tissue macrophage
RXR	retinoid X receptor
YS	yolk sac

REFERENCES

1. Blériot C, Chakarov S, and Ginhoux F. 2020. Determinants of resident tissue macrophage identity and function. Immunity 52: 957–970. [PubMed: 32553181]
2. Lavin Y, Mortha A, Rahman A, and Merad M. 2015. Regulation of macrophage development and function in peripheral tissues. Nat. Rev. Immunol 15: 731–744. [PubMed: 26603899]
3. Mass E, Ballesteros I, Farlik M, Halbritter F, Günther P, Crozet L, Jacome-Galarza CE, Händler K, Klughammer J, Kobayashi Y, et al. 2016. Specification of tissue-resident macrophages during organogenesis. Science 353: aaf4238. [PubMed: 27492475]
4. Evans RM, and Mangelsdorf DJ. 2014. Nuclear receptors, RXR, and the Big Bang. Cell 157: 255–266. [PubMed: 24679540]
5. Dawson MI, and Xia Z. 2012. The retinoid X receptors and their ligands. Biochim. Biophys. Acta 1821: 21–56. [PubMed: 22020178]

Author Manuscript Author Manuscript Author Manuscript Author Manuscript

6. Rőszer T, Menéndez-Gutiérrez MP, Cedenilla M, and Ricote M. 2013. Retinoid X receptors in macrophage biology. Trends Endocrinol. Metab 24: 460–468. [PubMed: 23701753]
7. Núñez V, Alameda D, Rico D, Mota R, Gonzalo P, Cedenilla M, Fischer T, Boscá L, Glass CK, Arroyo AG, and Ricote M. 2010. Retinoid X receptor α controls innate inflammatory responses through the up-regulation of chemokine expression. Proc. Natl. Acad. Sci. USA 107: 10626–10631. [PubMed: 20498053]
8. Rőszer T, Menéndez-Gutiérrez MP, Lefterova MI, Alameda D, Núñez V, Lazar MA, Fischer T, and Ricote M. 2011. Autoimmune kidney disease and impaired engulfment of apoptotic cells in mice with macrophage peroxisome proliferator-activated receptor γ or retinoid X receptor α deficiency. J. Immunol 186: 621–631. [PubMed: 21135166]
9. Ma F, Liu SY, Razani B, Arora N, Li B, Kagechika H, Tontonoz P, Núñez V, Ricote M, and Cheng G. 2014. Retinoid X receptor α attenuates host antiviral response by suppressing type I interferon. Nat. Commun 5: 5494. [PubMed: 25417649]
10. Casanova-Acebes M, Menéndez-Gutiérrez MP, Porcuna J, Álvarez-Errico D, Lavin Y, García A, Kobayashi S, Le Berichel J, Núñez V, Were F, et al. 2020. RXRs control serous macrophage neonatal expansion and identity and contribute to ovarian cancer progression. Nat. Commun 11: 1655. [PubMed: 32246014]
11. Liu Z, Gu Y, Shin A, Zhang S, and Ginhoux F. 2020. Analysis of myeloid cells in mouse tissues with flow cytometry. STAR Protoc 1: 100029. [PubMed: 33111080]
12. Ennamorati M, Vasudevan C, Clerkin K, Halvorsen S, Verma S, Ibrahim S, Prosper S, Porter C, Yeliseyev V, Kim M, et al. 2020. Intestinal microbes influence development of thymic lymphocytes in early life. Proc. Natl. Acad. Sci. USA 117: 2570–2578. [PubMed: 31964813]
13. Chen J, Kubalak SW, and Chien KR. 1998. Ventricular muscle-restricted targeting of the RXRalpha gene reveals a non-cell-autonomous requirement in cardiac chamber morphogenesis. Development 125: 1943–1949. [PubMed: 9550726]
14. Shimshek DR, Kim J, Hübner MR, Spergel DJ, Buchholz F, Casanova E, Stewart AF, Seeburg PH, and Sprengel R. 2002. Codon-improved Cre recombinase (iCre) expression in the mouse. Genesis 32: 19–26. [PubMed: 11835670]
15. Ogilvy S, Metcalf D, Gibson L, Bath ML, Harris AW, and Adams JM. 1999. Promoter elements of *vav* drive transgene expression in vivo throughout the hematopoietic compartment. Blood 94: 1855–1863. [PubMed: 10477714]
16. Chen MJ, Yokomizo T, Zeigler BM, Dzierzak E, and Speck NA. 2009. Runx1 is required for the endothelial to haematopoietic cell transition but not thereafter. Nature 457: 887–891. [PubMed: 19129762]
17. Okreglicka K, Iten I, Pohlmeier L, Onder L, Feng Q, Kurrer M, Ludewig B, Nielsen P, Schneider C, and Kopf M. 2021. PPARγ is essential for the development of bone marrow erythroblastic island macrophages and splenic red pulp macrophages. J. Exp. Med 218: e20191314. [PubMed: 33765133]
18. Schneider C, Nobs SP, Kurrer M, Rehrauer H, Thiele C, and Kopf M. 2014. Induction of the nuclear receptor PPAR-γ by the cytokine GM-CSF is critical for the differentiation of fetal monocytes into alveolar macrophages. Nat. Immunol 15: 1026–1037. [PubMed: 25263125]
19. Guilliams M, De Kleer I, Henri S, Post S, Vanhoutte L, De Prijck S, Deswarte K, Malissen B, Hammad H, and Lambrecht BN. 2013. Alveolar macrophages develop from fetal monocytes that differentiate into long-lived cells in the first week of life via GM-CSF. J. Exp. Med 210: 1977–1992. [PubMed: 24043763]
20. Ginhoux F, Greter M, Leboeuf M, Nandi S, See P, Gokhan S, Mehler MF, Conway SJ, Ng LG, Stanley ER, et al. 2010. Fate mapping analysis reveals that adult microglia derive from primitive macrophages. Science 330: 841–845. [PubMed: 20966214]
21. Ginhoux F, and Merad M. 2010. Ontogeny and homeostasis of Langerhans cells. Immunol. Cell Biol 88: 387–392. [PubMed: 20309014]
22. Gautier EL, Chow A, Spanbroek R, Marcelin G, Greter M, Jakubzick C, Bogunovic M, Leboeuf M, van Rooijen N, Habenicht AJ, et al. 2012. Systemic analysis of PPARγ in mouse macrophage populations reveals marked diversity in expression with critical roles in resolution of inflammation and airway immunity. J. Immunol 189: 2614–2624. [PubMed: 22855714]

Author Manuscript Author Manuscript Author Manuscript Author Manuscript

23. Gomez Perdiguero E, Klapproth K, Schulz C, Busch K, Azzoni E, Crozet L, Garner H, Trouillet C, de Bruijn MF, Geissmann F, and Rodewald HR. 2015. Tissue-resident macrophages originate from yolk-sac-derived erythromyeloid progenitors. Nature 518: 547–551. [PubMed: 25470051]

24. Hoeffel G, Chen J, Lavin Y, Low D, Almeida FF, See P, Beaudin AE, Lum J, Low I, Forsberg EC, et al. 2015. c-Myb^{+} erythromyeloid progenitor-derived fetal monocytes give rise to adult tissue-resident macrophages. Immunity 42: 665–678. [PubMed: 25902481]

25. Sheng J, Ruedl C, and Karjalainen K. 2015. Most tissue-resident macrophages except microglia are derived from fetal hematopoietic stem cells. Immunity 43: 382–393. [PubMed: 26287683]

26. Schulz C, Gomez Perdiguero E, Chorro L, Szabo-Rogers H, Cagnard N, Kierdorf K, Prinz M, Wu B, Jacobsen SE, Pollard JW, et al. 2012. A lineage of myeloid cells independent of Myb and hematopoietic stem cells. Science 336: 86–90. [PubMed: 22442384]

27. Cox N, Pokrovslki M, Vicario R, and Geissmann F. 2021. Origins, biology, and diseases of tissue macrophages. Annu. Rev. Immunol 39: 313–344. [PubMed: 33902313]

28. Gritz E, and Hirschi KK. 2016. Specification and function of hemogenic endothelium during embryogenesis. Cell. Mol. Life Sci 73:1547–1567. [PubMed: 26849156]

29. Mora JR, Iwata M, and von Andrian UH. 2008. Vitamin effects on the immune system: vitamins A and D take centre stage. Nat. Rev. Immunol 8: 685–698. [PubMed: 19172691]

Author Manuscript Author Manuscript Author Manuscript Author Manuscript

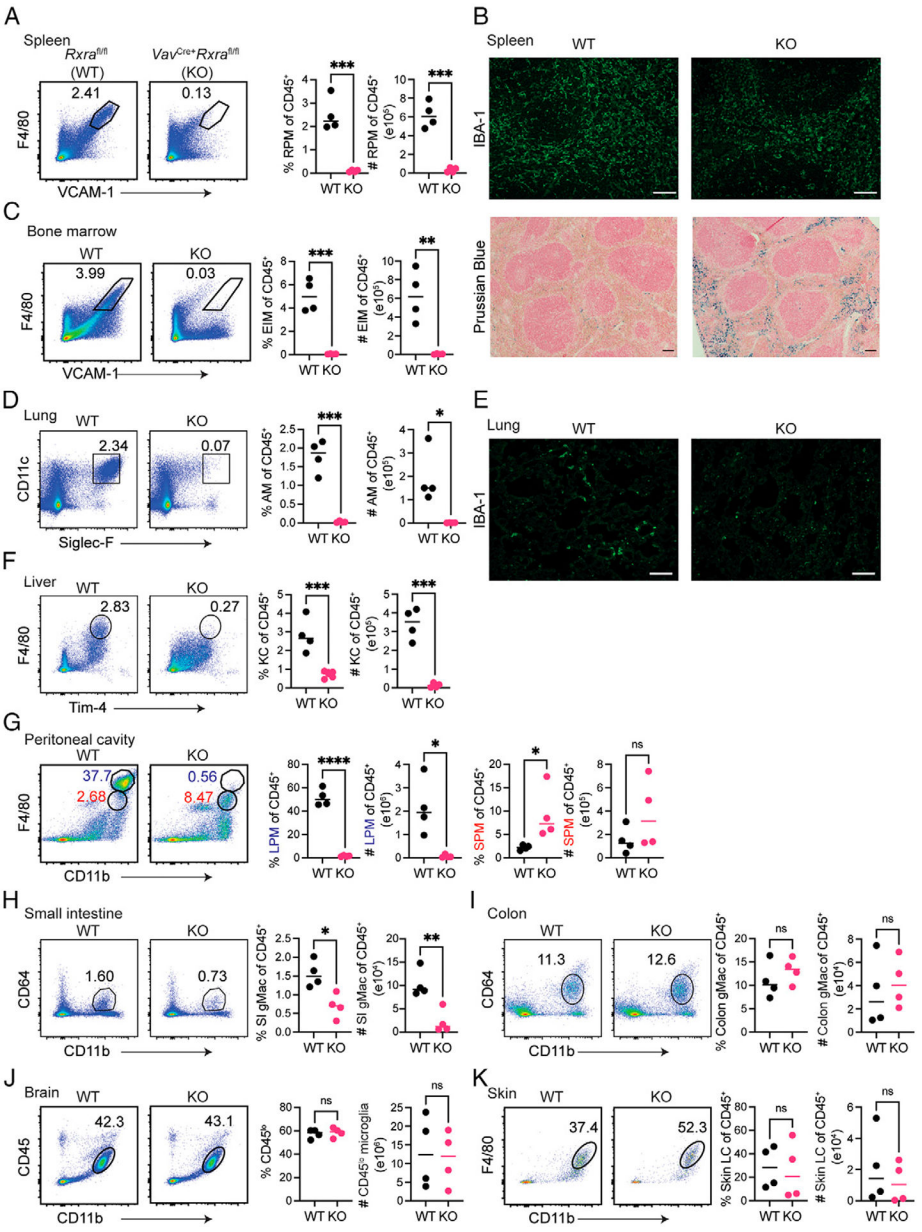

FIGURE 1. RXRα deficiency impacts multiple RTM subsets.

Analyses of RTM subsets from 8- 10-wk-old *Rxra*$^{fl/fl}$ (wild-type [WT]) and *Vav*$^{Cre+}$*Rxra*$^{fl/fl}$ (knockout [KO]) mice. Flow cytometry gating strategies are shown in Supplemental Fig. 2. (**A**) Representative flow cytometry dot plots and graphs show frequency and cell numbers among CD45^{+} cells of splenic red pulp macrophages (RPMs) (CD11b^{lo}F4/80^{hi}VCAM1^{+}), (**B**) Upper row, Immunohistochemistry staining of IBA-1 (pan-macrophage marker) on splenic sections. White scale bars, 50 μm. Bottom row, Representative microscopy image of splenic sections showing iron deposits by Prussian blue stain. Black scale bars, 25 μm. (**C**) Representative flow cytometry dot plots and graphs show frequency and cell numbers among CD45^{+} cells of bone marrow erythroblastic island macrophages (EIMs) (CD11b^{lo}F4/80^{hi}VCAM1^{+}). (**D**) Representative flow cytometry dot plots and graphs

Author Manuscript Author Manuscript Author Manuscript Author Manuscript

show frequency and cell numbers among $CD45^+$ cells of lung alveolar macrophages (AMs) ($CD11c^+Siglec\text{-}F^+$). (**E**) Immunohistochemistry staining of IBA-1 (pan-macrophage marker) on lung sections. Scale bars, 50 μm. (**F–K**) Representative flow cytometry dot plots and graphs show frequency and cell numbers among $CD45^+$ cells of (F) liver Kupffer cells (KCs) ($F4/80^+Tim4^+CD11b^+CD68^+$), (G) large and small peritoneal cavity macrophages (LPMs, SPMs) ($CD11b^+F4/80^{hi}$ and $CD11b^+F4/80^{lo}$), (H) small intestine macrophages (SI gMacs) ($CD11b^+CD64^+CD11c^{lo}F4/80^+$) (I) large intestine macrophages (Colon gMacs) ($CD11b^+CD64^+CD11c^{lo}F4/80^+$), (J) brain microglia ($CD45^{lo}CD11b^+$), and (K) skin Langerhans cells (LCs) ($CD11b^+F4/80^+$). Data are representative of three independent experiments. Error bars are SEM. *$p < 0.05$, **$p < 0.01$, ***$p < 0.001$, ****$p < 0.0001$.

Author Manuscript Author Manuscript Author Manuscript Author Manuscript

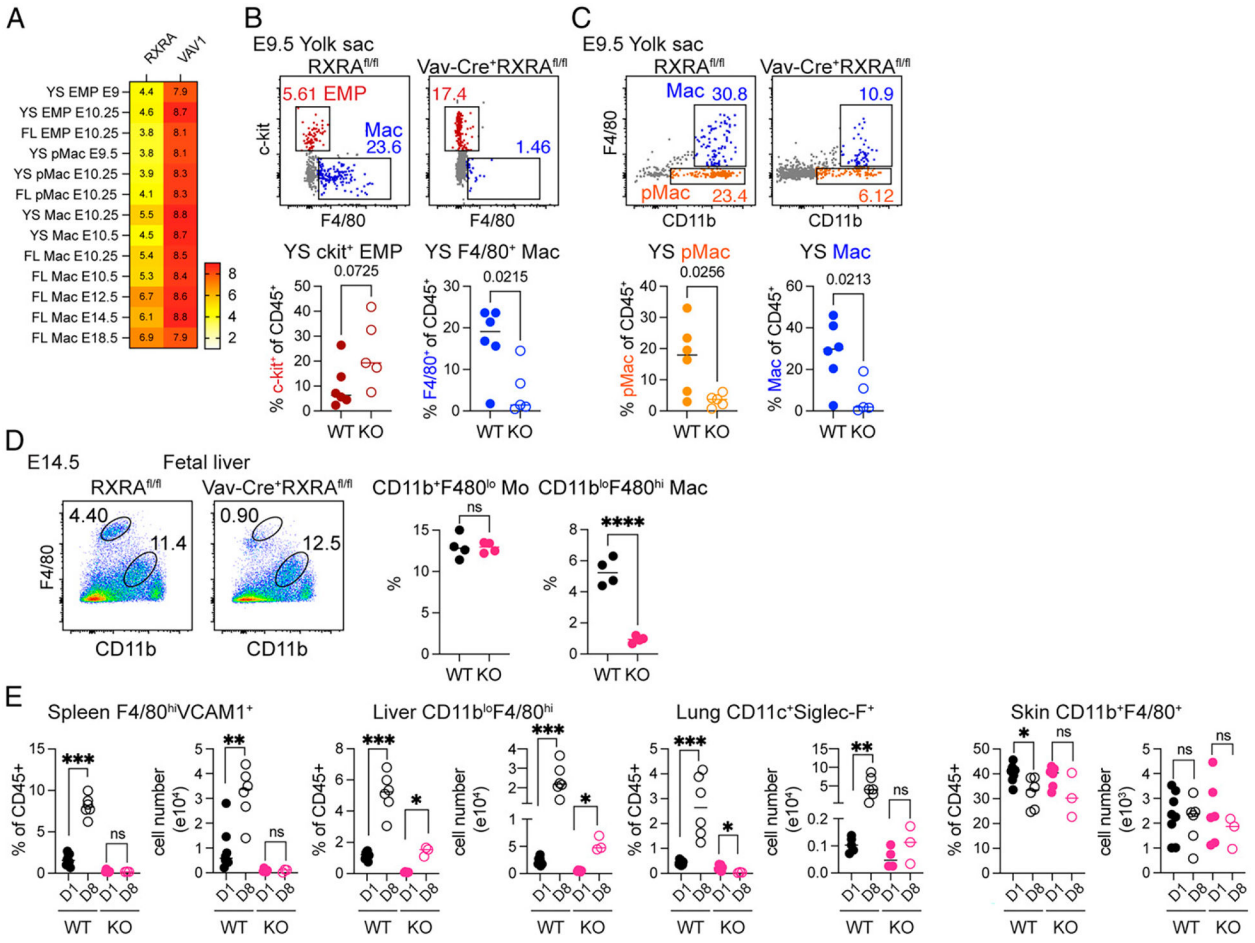

FIGURE 2. RXRα deficiency impacts embryonic development of RTMs.

(**A**) RNA-seq dataset from Mass et al. (3) were analyzed for the expression of *Rxra* and *Vav1.* Heatmaps show normalized gene expression ($\log_2$) of transcripts for *Rxra* (average of ENSMUST00000077257, ENSMUST00000100251, ENSMUST00000166775) and *Vav1* (average of ENSMUST00000169220, ENSMUST00000005889, ENSMUST00000112870). (**B** and **C**) Flow cytometry analyses of E9.5 yolk sac (YS) from *Rxra*$^{fl/fl}$ (wild-type [WT]) and *Vav*$^{Cre+}$*Rxra*$^{fl/fl}$ (knockout [KO]) embryos. (B) Representative dot plots and graphs show frequency among CD45$^+$ cells of EMPs (CD45$^+$c-Kit$^+$) and macrophages (CD45$^+$F4/80$^+$). Phenotypes of c-Kit$^+$ and F4/80$^+$ cells are detailed further in Supplemental Fig. 3. (C) Representative dot plots and graphs show frequency among CD45$^+$ cells of precursor macrophages (pMacs) (CD45$^+$CD11b$^{lo/+}$F4/80$^-$) and macrophages (Macs) (CD45$^+$CD11b$^+$F4/80$^+$). (**D**) Flow cytometry analyses of E14.5 fetal liver (FL) from *Rxra*$^{fl/fl}$ (WT) and *Vav*$^{Cre+}$*Rxra*$^{fl/fl}$ (KO) fetuses. Representative flow cytometry dot plots and graphs show frequency among CD45$^+$ cells of E14.5 FL monocytes (CD45$^+$CD11b$^+$F4/80^{lo} Mos) and macrophages (CD45$^+$CD11b^{lo}F4/80^{hi} Macs). Data in (B)–(D) are from two independent experiments. (**E**) Frequency and cell numbers among CD45$^+$ cells of postnatal day 1 (D1) and 8 (D8) spleen (F4/80$^+$VCAM1$^+$), liver (CD11b^{lo}F4/80^{hi}), lung (CD11c$^+$Siglec-F$^+$) and

skin ($CD11b^{+}F4/80^{+}$) RTM subsets. Data in (E) are representative of three independent experiments. Error bars are SEM. *$p < 0.05$, **$p < 0.01$, ***$p < 0.001$, ****$p < 0.0001$.

Author Manuscript Author Manuscript Author Manuscript Author Manuscript